High repetition rate plasma mirror device for attosecond science

A. Borot, D. Douillet, G. Iaquaniello, T. Lefrou, P. Audebert, J.-P. Geindre, and R. Lopez-Martens

High repetition rate plasma mirror device for attosecond science

A. Borot,[1] D. Douillet,[1] G. Iaquaniello,[1] T. Lefrou,[1] P. Audebert,[2] J.-P. Geindre,[2] and R. Lopez-Martens[1]

[1]*Laboratoire d'Optique Appliquée, ENSTA-ParisTech, CNRS, Ecole Polytechnique, UMR 7639, 91761 Palaiseau, France*
[2]*Laboratoire pour l'Utilisation des Lasers Intenses, Ecole Polytechnique, CNRS, 91128 Palaiseau Cedex, France*

This report describes an active solid target positioning device for driving plasma mirrors with high repetition rate ultra-high intensity lasers. The position of the solid target surface with respect to the laser focus is optically monitored and mechanically controlled on the *nm* scale to ensure reproducible interaction conditions for each shot at arbitrary repetition rate. We demonstrate the target capabilities by driving high-order harmonic generation from plasma mirrors produced on glass targets with a near-relativistic intensity few-cycle pulse laser system operating at 1 kHz. During experiments, residual target surface motion can be actively stabilized down to 47 nm (root mean square), which ensures sub-300-as relative temporal stability of the plasma mirror as a secondary source of coherent attosecond extreme ultraviolet radiation in pump-probe experiments. © *2014 AIP Publishing LLC*. [http://dx.doi.org/10.1063/1.4860035]

I. INTRODUCTION

When an intense femtosecond pulse ($I > 10^{16}$ W/cm^2) hits an optically polished solid surface, it generates a dense plasma that itself acts as a mirror, known as a plasma mirror (PM).[1] PMs do not just reflect the remainder of the incident beam, but can act as active optical elements that can be used for improving the temporal contrast of modern ultra-high intensity lasers[2,3] with 70%-80% efficiency, or generating intense attosecond extreme ultraviolet (XUV) or X-ray pulses through nonlinear harmonic upconversion of the laser frequency.[4–6] PMs are currently foreseen as a new generation of attosecond light sources, potentially delivering keV photon bunches energies with unprecedented efficiency and duration when driven at ultra-high intensity ($\simeq 10^{20}$ W/cm^2).[12] So far, most PM experiments have been performed using large scale laser systems delivering typical pulse energies in the range 1–10 J on a single-shot basis or at a few Hz only. A much less explored regime consists in tightly focusing milliJoule-energy laser pulses down to wavelength-scale spot sizes in order to drive PMs using kHz laser technology.[7–10] This regime recently allowed, for the first time, attosecond time scale control of PM dynamics driven by waveform-controlled few-cycle light fields with near-relativistic intensity.[11] Such experiments offer the exciting prospects of producing intense isolated XUV attosecond pulses in the fully relativistic regime[12–14] and at high repetition rates for attosecond science applications.[15]

Driving PMs at kHz repetition rate with tightly focused femtosecond pulses offers many advantages for applications but also presents some serious technical challenges. First let us consider the advantages. Operating at kHz rate provides almost instant access to the statistics of the underlying highly nonlinear laser-plasma interaction process. This in turn allows quick and systematic online optimization of plasma mirror and secondary (attosecond) beam parameters, such as pulse duration, spectral range, spatial profile, and divergence. A direct consequence of this is that it also makes it possible to observe systematic trends in the variation of the temporal attosecond source properties as a function of the driving laser waveform,[10,11] through pulse averaging, which simply cannot be accessed directly with lower repetition rate laser systems. Now let us consider the technical challenges. Plasma mirrors require the laser to be focused onto a solid with optical grade surface quality. As the interaction zone is destroyed after every laser shot, the target surface must therefore be refreshed at the laser repetition rate while maintaining identical interaction conditions from shot to shot. This means that the position (depth and orientation) of the target surface relative to the laser focus plane must be carefully controlled during the experiment to avoid significant intensity fluctuations. In practical terms, target misalignment during the refreshment process must remain small compared to the Rayleigh length of the focused laser beam, which in the case of fast focusing of optical pulses, is significantly less than 10 μm. Today, a typical attosecond time-resolved pump-probe experiment requires a relative stability between the pump and probe light fields less than 300 as over a period of several tens of minutes. A light source based on a kHz-driven plasma mirror therefore becomes useful for attosecond applications if the shot-to-shot target surface fluctuations are kept well below 100 nm over sufficiently large surface areas in order to support several million consecutive laser shots.

II. ROTATING/TRANSLATING TARGET HOLDER FOR DRIVING kHz PLASMA MIRRORS

We have developed an optical target positioning device that allows plasma mirror operation at kHz rate under vacuum for attosecond applications in the XUV spectral range.[10,11,14] It features an all-optical technique for online monitoring of
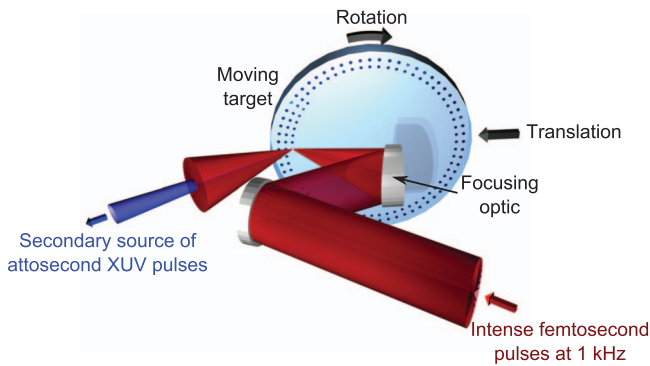
FIG. 1. Scheme of the high-repetition rate laser-solid target interaction setup, with circular impact pattern interaction geometry. The target rotates clockwise and translates toward the left.
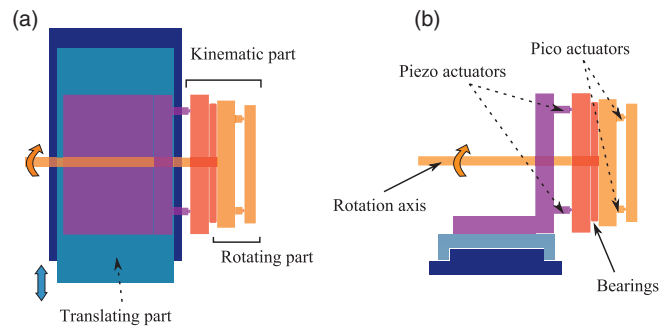

FIG. 2. Schematic of the high-repetition rate laser-solid target holder, (a) in top view and (b) in side view. The rotating part of the target holder (light orange) is linked to a non-rotating part (dark orange) by means of a roller bearing. This whole sub-assembly is fixed onto a frame (purple) that can be kinematically displaced using a set of three piezo actuators. The frame sits on a translation stage (light and dark blue).

the target surface position, which in turn allows active stabilization of large surface area targets below 50 nm root mean square (RMS) for the delivery of the secondary laser-driven plasma mirror emission to attosecond experiments over several million consecutive shots with sub-300 as relative stability. The stability afforded by the device is demonstrated both through interferometric measurement of target surface fluctuations and through multi-shot spectral and spatial averaging of high-order harmonic emission from a plasma mirror driven at kHz rate using waveform-controlled few-cycle laser pulses.

The device consists of a rotating/translating target holder (Fig. 1) featuring a 14 cm diameter flat optical substrate as the target. The target surface is positioned vertically with respect to the laser plane at a chosen laser incidence angle. In order to maximize the number of consecutive shots per target face, the substrate is rotated over a full period, drawing a circle of impacts on the surface, after which it is translated in order to draw a second circle of impacts concentric with the previous one. This shot pattern is then repeated across the entire target surface, which provides an approximate number of shots per target $N = \pi R^2 / a^2$, where R is the radius of the target and a is the distance between each shot. For instance, using a mJ pulse energy kHz laser[10] and assuming a 100 μm distance between each shot to avoid debris, a 14 cm diameter target ensures up to 1.5 million consecutive shots per face, which equates to 25 min of continuous operation at 1 kHz.

A rotating/translating target geometry rather than simple rectangular target translation for instance is preferable for

several reasons: first, the former ensures minimal space around the target holder allocated for target displacement during kHz operation in comparison with a rectangular target of same surface area. Second, it allows the target to move continuously without brutal acceleration or deceleration during the motion, contrary to the fully translated geometry. The rotation of the target is ensured by high-load axial/radial roller bearings (Schaeffler Technologies). Because such high-precision bearings have a high torque due to friction, a high torque rotor motor (Mitsubishi Electric) is placed outside the vacuum chamber in order to dissipate heat and reduce on-axis vibrations. As the target holder must work for any configuration inside the vacuum chamber, the motor and bearing transmission axes are decoupled through a double-universal joint connector, where the two axes can slide freely with respect to each other in the longitudinal direction. This allows arbitrary orientation of the target surface rotation axis with respect to the motor axis. The target holder then sits on a motorized high-load long-range translation stage (Schneeberger) in order to radially scan the target surface. Schematics and Computer-Aided-Design (CAD) drawings of the device are presented, respectively, in Figs. 2 and 3.

The target rotation speed is set by the minimal acceptable distance between consecutive laser shots (empirically determined via target surface inspection using a microscope), the laser repetition rate, and the radial position of the focus with respect to the target center. It can be expressed as
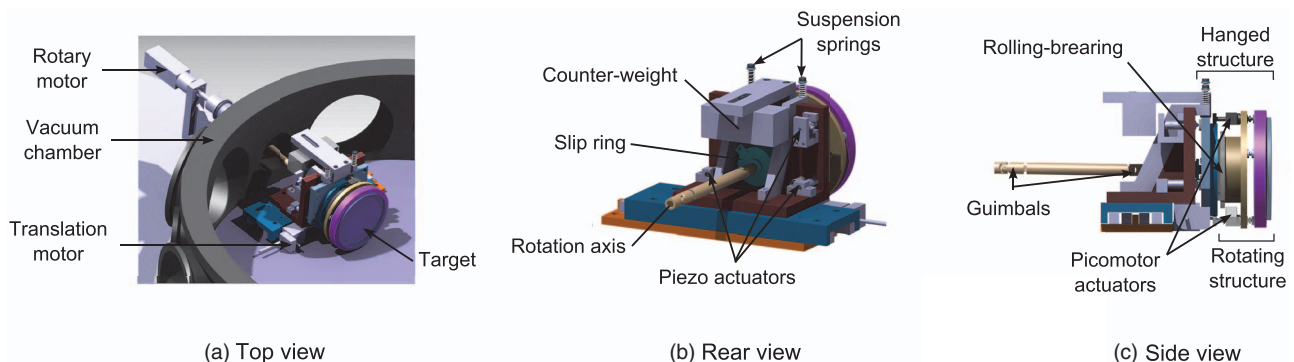

FIG. 3. Computer-Aided-Design (CAD) drawing of the high-repetition rate target holder: top view (a), rear view (b), and side view (c).

$\Omega = va/R$, where Ω, where v the laser repetition rate. This speed increases as the laser-plasma interaction is driven closer to the target center. The minimal translation step is set by the minimum distance between concentric shot patterns, which is itself determined by the minimal acceptable distance between consecutive shots. In the present device, a computerized user interface controls the target motion (rotation and translation), the interaction parameters (laser repetition rate, shot spacing, focus position on target, etc.), and the mode of operation (burst mode or continuous mode). The optimal target motion sequence is then calculated and transmitted to the rotation and translation motors according to the shot pattern chosen by the user.

III. INTERFEROMETRIC MONITORING OF TARGET POSITION

Previously, we stressed the need for precise monitoring of the target surface in order to stabilize fluctuations of its position relative to the laser focus. However, this monitoring must be non-invasive during experiments. Optical interferometry provides excellent spatial resolution and does not intrude in the interaction area. As a light source for the interferometer, we use a Helium-Neon (He-Ne) laser (Melles-Griot) with active frequency stabilization (frequency drift $<\pm 3$ MHz per month) with minimal longitudinal and transverse mode beating, which improves the stability of spatial interference fringes and hence the ultimate resolution of the interferometric measurement. It also provides a coherence length of several hundred of meters, which allows the use of highly unbalanced interferometer arms and therefore total flexibility in the layout of the interferometer around the target holder. The He-Ne beam is first expanded to 1 cm diameter beam and sent into the vacuum chamber, sitting on the same optical table (vibrations resulting from vacuum pumping must be mechanically decoupled from experiments). The beam is then sent into a Mach-Zehnder interferometer, one arm reflected off an unused portion of the target face and the other off a fixed mirror in the vacuum chamber (Fig. 4(a)). Both arms are then spatially recombined with a small angle in the horizontal plane, generating a vertical parallel interference pattern (Fig. 4(b)). The fringe contrast is maximized by appropriately balancing beam intensities in both arms of the interferometer, depending on the reflectivity of the chosen target material. A Charge-Coupled Device (CCD) camera placed outside the vacuum chamber records the interference pattern online. All the optics used in the setup exhibit $\lambda/20$ surface flatness for 633 nm light. As the target rotates, the relative displacement of the target face induces a change in the interference pattern: A change in depth (horizontal displacement) leads to a lateral shift of the fringe pattern (Fig. 4(c)); a change in the tangential angle (vector normal to the surface moving in the vertical plane) leads to a tilt of the fringe pattern (Fig. 4(d)); a change in the azimuthal angle (vector normal to the surface moving in the horizontal plane) changes the fringe spacing (Fig. 4(e)).

During operation, the real motion of the target surface is retrieved by online spatial Fourier analysis of the fringe pattern recorded by the CCD. Each consecutive CCD frame provides a measure of the relative change in target
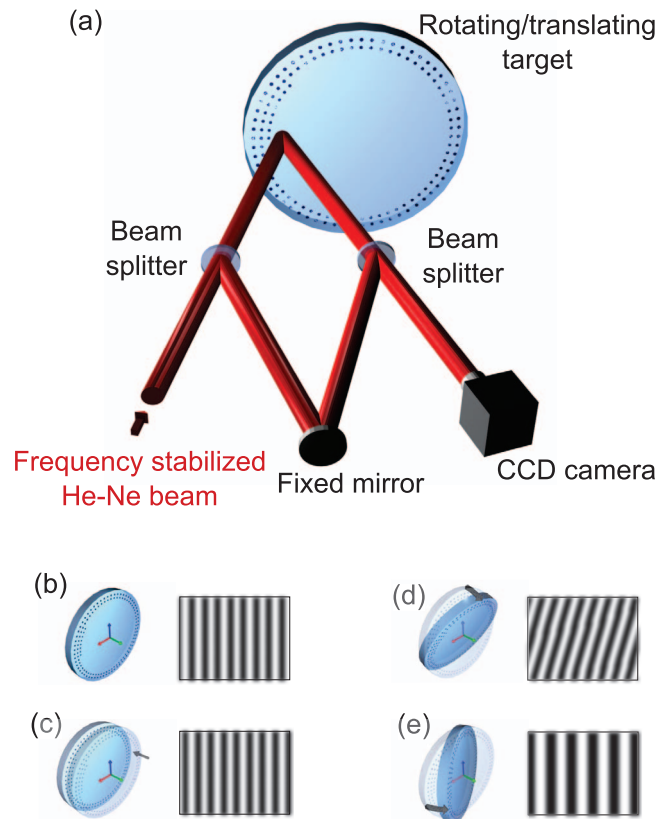

FIG. 4. Schematic of the Mach-Zehnder interferometer used for optical monitoring of target surface motion (a). Typical interference fringes' patterns observed as a result of a change in depth (c), in latitude (d), and azimuth (e) of the target surface with respect to an initial position (b).

position. Fringe analysis can be performed at high repetition rate (100 Hz) using small image frames (100×50 pixels) without any loss of resolution. A crucial point has to be raised here: although changes in target orientation (tangential and azimuthal angles) can be unambiguously retrieved, longitudinal displacements cannot if in between frames the beam path in the target interferometer arm shifts by more than a He-Ne laser wavelength (632 nm). This underlines the importance of fast acquisition and processing of the fringe pattern during target operation.

IV. PASSIVE TARGET STABILIZATION

We can now use this online monitoring technique to minimize the relative motion of the target surface. First, we minimize precession of the vector normal to the target face with respect to the rotation axis of the bearings. This so-called static alignment is done using two diametrically opposed picomotor piezo linear actuators placed on the rotating assembly of the target holder, providing sub-μrad control over the precession angle. Fig. 5 shows the residual periodic target motion recorded over several target revolutions, after precession has been minimized (these measurements were taken at the outer edge of the target where precession is greatest and are therefore considered to be an upper limit in stability). Target surface motion is limited to 1.9 μm peak-to-valley (PTV) in depth (360 nm RMS) and 100 μrad PTV in orientation (29 μrad RMS). It is interesting to notice the double
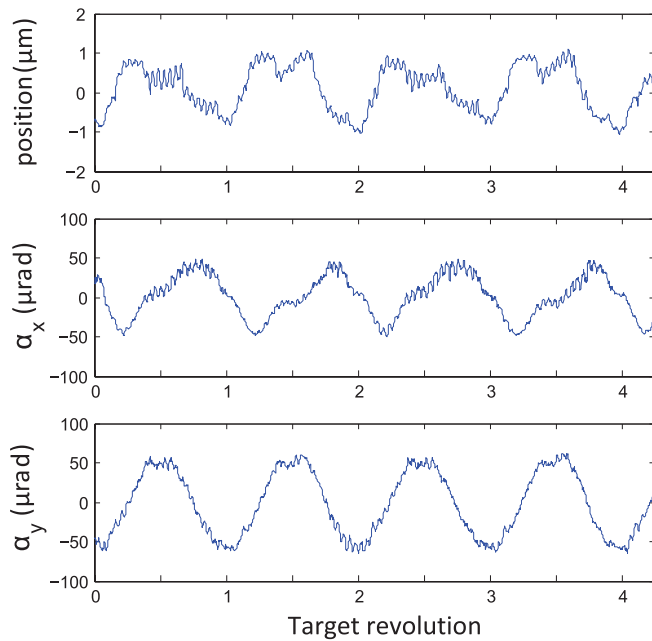
FIG. 5. Typical target positioning performance following static prealignment. Residual motion in depth (d), azimuth (α_x), and latitude (α_y) is measured over four full target revolutions.
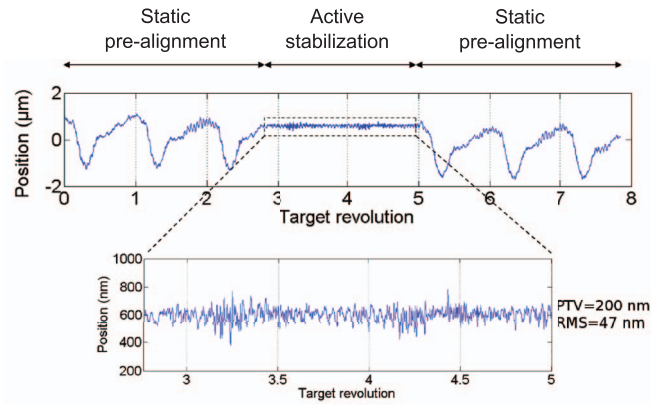

FIG. 6. Typical target positioning performance using online active stabilization of the target surface motion. Stabilization is successively activated and deactivated to compare with passive alignment performance.

periodicity of the residual target motion with respect to the target revolution. This comes from the fact that the cylindrical rollers inside the bearings execute a full rotation over two full target revolutions. Residual target motion is now limited only by the mechanical tolerance of the bearings and the target surface quality.

V. ACTIVE TARGET STABILIZATION

Active target stabilization is now needed in order to achieve attosecond optical precision. The structure comprising the bearing and the rotating assembly is mounted onto a frame that can be controlled kinematically using a set of three preloaded linear piezo actuators. The range of the piezo actuators is chosen to be 35 μm, which is enough to correct the residual motion of ≈ 2 μm obtained after static prealignment (see Fig. 5). Although piezoelectric motors can push heavy charges at high repetition rate, care must be taken not to apply lateral force or torque on the actuators. To avoid this, two gallows combined with suspension springs are used to support the translation assembly. A counter weight then balances the assembly so that no lateral forces are applied on the piezo motors. The contact between the translating assembly and the piezo motors is ensured by a set of three counter balance springs.

The set of piezo motors is then used to actively feedback on the minimize residual target motion as it rotates and translates after each interferometric measurement. Each camera frame is analyzed and provides the change in depth and orientation angles of the target surface. These changes are then corrected online using the piezo actuators. Fig. 6 compares target stabilization with and without online correction of the depth, over 8 target revolutions. When using active stabilization, relative fluctuations in target surface depth are

brought down to 400 nm peak-to-valley with a standard deviation of 47 nm. Feedback to the piezo-actuators is done at 30 Hz repetition rate, for a local target velocity of a few cm/s. Active stabilization therefore improves target surface stability by almost a factor of ten, bringing the temporal stability of the PM surface as an optical source down to below 300 as.

VI. HIGH-HARMONIC GENERATION FROM A kHz PLASMA MIRROR

The overall device performance was characterized by driving high-order harmonic generation from plasma mirrors rate using a kHz femtosecond laser system. The setup used to characterize the emission of coherent XUV radiation generated off the kHz-driven plasma mirrors is presented in Fig. 7 and more details are available in Ref. 10. The laser beam is tightly focused with a 1.7 numerical aperture off-axis parabola onto the fused silica target surface at intensities of the order of a few 10^{17} W cm^{-2}. At these intensities, the laser-plasma interaction leads the production of a train of attosecond pulses in the XUV spectral range.[6] We characterize this XUV radiation spectrally by using a non-imaging spectrometer, and spatially by introducing a detector directly into the path of the beam reflected off the plasma mirror. The acquisition sequence is the following: the laser beam is first blocked by an ultrafast mechanical shutter, the motion of the target is launched until it reaches the end of the acceleration stage, then the shutter is opened, allowing a tight sequence of plasma mirrors to be generated on the target surface at kHz repetition rate. The duration of the laser-target interaction is set by the user. The spectral or spatial signal is then integrated over the chosen number of consecutive shots by tuning the acquisition time of the CCD camera on which the detector signals are imaged. Several integrated signals can then be successively acquired, while the target is still rotating and the shutter open. Once the acquisition is finished, the shutter is closed and the target motion is stopped. Figs. 7(i) and 7(j) show the typical spectrum and spatial profile of the XUV plasma mirror emission, acquired, respectively, over 100 and 30 laser shots. (In this case, the laser pulse duration driving the interaction was set to 27 fs full width at half maximum.)
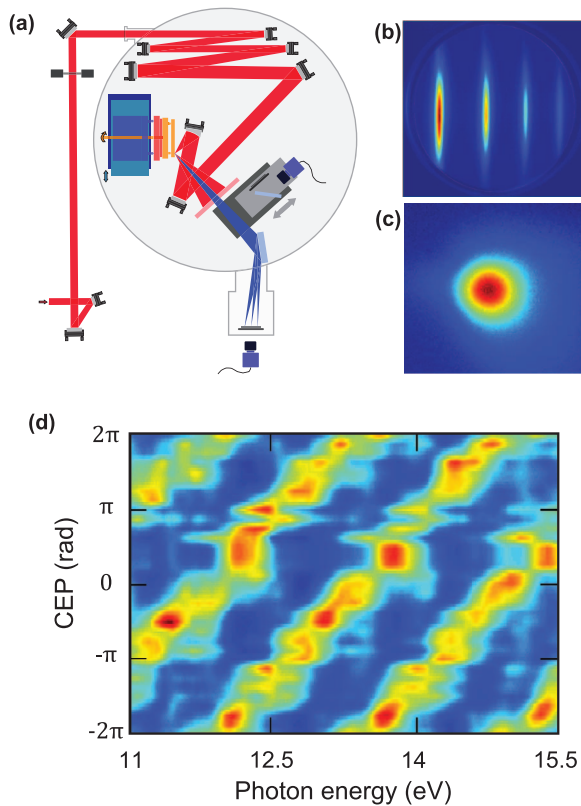
FIG. 7. Schematic of the spectral and spatial characterization of XUV harmonic emission from the kHz plasma mirror (a), with typical row measurements of spectrum (b) and spatial profile (c) when driven with 27 fs pulses. (d) A map of computed XUV spectra (each integrated over 300 consecutive shots) taken for 64 consecutive values of laser CEP, when driven by waveform-controlled 5 fs laser pulses.

In a second experiment, we observe the variation of the harmonic emission spectrum of the PM driven at 1 kHz by two-cycle (5 fs at 800 nm) laser pulses with controlled waveform, i.e., with controlled carrier-to-envelope phase (CEP).[11] Minimizing the CEP drift of such pulses (drift of the laser field oscillations with respect to the pulse intensity envelope) can only be achieved in practice over short times, typically less than one hour. This implies that a systematic CEP-dependent measurement must be done within the same amount of time. Measuring the harmonic spectrum as a function of laser CEP requires scanning over a large range of CEP values (typically 50 different values for a temporal resolution of 50 as), while integrating each spectrum over a very large number of shots. In Fig. 7(d), we show a map of the variation of the harmonic spectrum measured over a 4π rad range of relative CEP values. Each spectrum is integrated over 300 shots and 64 spectra are computed in order to obtain this map,

which corresponds to 20 000 shots in total. At 1 kHz repetition rate, this experiment takes half an hour to perform, while it would have demanded over an entire day using a 10 Hz laser system, for which CEP stabilization has not yet been demonstrated.

VII. CONCLUSION

We report here the first technical solution for driving plasma mirrors at ultra-high intensity using a kHz femtosecond laser system. A large surface target is rotated and translated during the interaction, while the target surface is monitored online by interferometry. Passive prealignment ensures a motion of 310 nm RMS in depth and 25 μrad RMS in angle over the interaction area. The depth position of the target surface can also be actively stabilized down to 47 nm RMS, which ensures sub-300 as temporal resolution in pump-probe experiments where the PM emission is used as a secondary source of attosecond pulses.

[1]H. C. Kapteyn, M. M. Murnane, A. Szoke, and R. W. Falcone, Opt. Lett. **16**, 490 (1991).
[2]G. Doumy, F. Quéré, O. Gobert, M. Perdrix, P. Martin, P. Audebert, J. C. Gauthier, J.-P. Geindre, and T. Wittmann, Phys. Rev. E **69**, 026402 (2004).
[3]B. Dromey, S. Kar, M. Zepf, and P. Foster, Rev. Sci. Instrum. **75**, 645 (2004).
[4]B. Dromey, M. Zepf, A. Gopal, K. Lancaster, M. S. Wei, K. Krushelnick, M. Tatarakis, N. Vakakis, S. Moustaizis, R. Kodama, M. Tampo, C. Stoeckl, R. Clarke, H. Habara, D. Neely, S. Karsch, and P. Norreys, Nat. Phys. **2**, 456 (2006).
[5]C. Thaury, F. Quere, J.-P. Geindre, A. Levy, T. Ceccotti, P. Monot, M. Bougeard, F. Reau, P. d'Oliveira, P. Audebert, R. Marjoribanks, and P. Martin, Nat. Phys. **3**, 424 (2007).
[6]Y. Nomura, R. Horlein, P. Tzallas, B. Dromey, S. Rykovanov, Z. Major, J. Osterhoff, S. Karsch, L. Veisz, M. Zepf, D. Charalambidis, F. Krausz, and G. D. Tsakiris, Nat. Phys. **5**, 124 (2009).
[7]O. Albert, H. Wang, D. Liu, Z. Chang, and G. Mourou, Opt. Lett. **25**, 1125 (2000).
[8]Y. Nomura, L. Veisz, K. Schmid, T. Wittmann, J. Wild, and F. Krausz, New J. Phys. **9**, 9 (2007).
[9]J. H. Easter, A. G. Mordovanakis, B. Hou, A. G. R. Thomas, J. A. Nees, G. Mourou, and K. Krushelnick, Opt. Lett. **35**, 3186 (2010).
[10]A. Borot, A. Malvache, X. Chen, D. Douillet, G. Iaquianiello, T. Lefrou, P. Audebert, J.-P. Geindre, G. Mourou, F. Quéré, and R. Lopez-Martens, Opt. Lett. **36**, 1461 (2011).
[11]A. Borot, A. Malvache, X. Chen, A. Jullien, J.-P. Geindre, P. Audebert, G. Mourou, F. Quere, and R. Lopez-Martens, Nat. Phys. **8**, 416 (2012).
[12]G. Tsakiris, K. Eidmann, J. Meyer-ter-Vehn, and F. Krausz, New J. Phys. **8**, 19 (2006).
[13]P. Heissler, R. Hörlein, J. M. Mikhailova, L. Waldecker, P. Tzallas, A. Buck, K. Schmid, C. M. S. Sears, F. Krausz, L. Veisz, M. Zepf, and G. D. Tsakiris, Phys. Rev. Lett. **108**, 235003 (2012).
[14]J. A. Wheeler, A. Borot, S. Monchoce, H. Vincenti, A. Ricci, A. Malvache, R. Lopez-Martens, and F. Quere, Nat. Photon. **6**, 829 (2012).
[15]F. Krausz and M. Ivanov, Rev. Mod. Phys. **81**, 163 (2009).